Polarization correlations in pulsed, vertical-cavity, surface-emitting lasers

D.R. Shelly, T.W.S. Garrison, M. Beck
Department of Physics, Whitman College, Walla Walla, Washington 99362
shellydr@whitman.edu, garristw@whitman.edu, beckmk@whitman.edu

D.H. Christensen
Department of Physics, University of Colorado, Boulder, Colorado 80309

Abstract: We have examined noise behavior and polarization correlations in the output of a pulsed, multitransverse-mode, vertical-cavity, surface-emitting laser (VCSEL). We have measured the output of the laser simultaneously in two orthogonal, linear polarizations as a function of drive current for pulse widths of 3 ns, 10 ns, and 30 ns. We present joint probability distributions for the number of detected photoelectrons in each of the two polarization-resolved outputs. The joint distributions indicate that the correlations can be quite complicated, and are not completely described by a single number (i.e., the correlation coefficient). Furthermore, we find that the number of lasing modes appears to be the most important parameter in determining the degree of polarization correlation.

OCIS codes: (250.7260) Vertical cavity surface emitting lasers; (140.5960) Semiconductor lasers

References and links

1. C. J. Chang-Hasnain, "Vertical-cavity surface emitting lasers," in *Semiconductor Lasers: Past, Present, and Future*, G. P. Agrawal, ed. (American Institute of Physics, Melville, N.Y., 1995), pp. 145-180.
2. F. Koyama, K. Morit, and K. Iga, "Intensity noise and polarization stability of GaAlAs-GaAs surface emitting lasers," IEEE J. Quantum Electron. **27**, 1410-1416 (1991).
3. T. Mukaihara, N. Ohnoki, Y. Hayashi, N. Hatori, F. Koyama, and K. Iga, "Excess intensity noise originated from polarization fluctuation in vertical-cavity surface-emitting lasers," IEEE Photon. Technol. Lett. **7**, 1113-1115 (1995).
4. D.C. Kilper, P.A. Roos, J.L. Carlsten, and K.L. Lear, "Squeezed light generated by a microcavity laser," Phys. Rev. A **55**, R3323-R3326 (1997).
5. M.P. van Exter, M.B. Willemsen, and J.P. Woerdman, "Polarization fluctuations in vertical-cavity semiconductor lasers," Phys. Rev. A **58**, 4191-4205 (1998).
6. G. Giacomelli, F. Martin, M. Gabrysch, K.H. Gulden, and M. Moser, "Polarization competition and noise properties of VCSELs," Opt. Comm. **146**, 136-140 (1998).
7. J.-L. Vey, C. Degen, K. Auen, and W. Elsäßer, "Quantum noise and polarization properties of vertical-cavity, surface-emitting lasers," Phys. Rev. A **60**, 3284-3295 (1999).
8. M.B. Willemsen, M.P. van Exter, and J.P. Woerdman, "Correlated fluctuations in the polarization modes of a vertical-cavity semiconductor laser," Phys. Rev. A **60**, 4105-4113 (1999).
9. D.V. Kuksenkov, H. Temkin, and S. Swirhun, "Polarization instability and relative intensity noise in vertical-cavity surface-emitting lasers," Appl. Phys. Lett. **67**, 2141-2143 (1995).
10. D.V. Kuksenkov, H. Temkin, and S. Swirhun, "Polarization instability and performance of free-space optical links based on vertical-cavity surface-emitting lasers," IEEE Photon. Technol. Lett. **8**, 703-705 (1996).
11. T.W.S. Garrison, M. Beck, and D.H. Christensen, "Noise behavior of pulsed vertical-cavity, surface-emitting lasers," J. Opt. Soc. Am. B **16**, 2124-2130 (1999).
12. K.D. Choquette, R.P. Schneider, and K.L. Lear, "Gain-dependent polarization properties of vertical cavity lasers," IEEE J. Select. Topics Quantum Electron. **1**, 661-666 (1995).
13. M. San Miguel, Q. Feng, and J.V. Molony, "Light-polarization dynamics in surface-emitting semiconductor lasers," Phys. Rev. A **52**, 1728-1739 (1995).

#23232 - $15.00 US Received August 01, 2000; Revised September 25, 2000

14. A. Valle, L. Pesquera, and K.A. Shore, "Polarization behavior of birefringent multitransverse mode vertical-cavity surface-emitting lasers," IEEE Photon. Tech. Lett. **9**, 557-559 (1997).
15. K. Panajotov, B. Kyvkin, J. Danckaert, M. Peeters, H. Thienpont, and I. Veretennicoff, "Polarization switching in VCSEL's due to thermal lensing," IEEE Photon. Tech. Lett. **10**, 6-8 (1998).
16. M Giudici, J.R. Tredicce, G. Vaschenko, J.J. Rocca, and C.S. Menoni, "Spatio-temporal dynamics in vertical cavity surface emitting lasers excited by fast electrical pulses," Opt. Comm. **158**, 313-321 (1998).
17. While quantum mechanics states that losses can significantly effect correlations between optical fields, we find that the measured noise levels of our fields are more than an order of magnitude above the shot-noise level. This means that the fields are well described by classical mechanics, and we do not anticipate that this additional loss will impact the results described here.
18. J.P. Hermier, A. Bramati, A.Z. Khoury, E. Giacobino, J.P. Poizat, T.J. Chang, P. Grangier, "Spatial quantum noise of semiconductor lasers," J. Opt. Soc. Am. B **16**, 2140-2146 (1999).

1. Introduction

Vertical-cavity, surface-emitting lasers (VCSELs) are microcavity semiconductor lasers which emit perpendicular to the substrate plane. Largely because of their small size, VCSELs exhibit a number of interesting properties: single-longitudinal mode output, low threshold-current, and high efficiency [1]. However, because of their circular symmetry, polarization selection is very weak in these lasers; consequently the output from a VCSEL is usually not polarized. The laser can lase in either one of two linear polarizations, or it can lase in both polarizations simultaneously, or it can undergo polarization switching. The details of this polarization behavior are not yet completely understood, and in the past few years there has been a great deal of interest, both experimental and theoretical, in this topic [2-15].

Many previous studies have examined noise and/or polarization behavior of VCSELs, but the vast majority of these experiments have been carried out on continuous-wave (CW) lasers [2-8], while very few have been done using pulsed lasers [9-11,16]. Here we examine the behavior of a pulsed VCSEL. Measurements of pulsed lasers are important for several reasons. Noise characterization of pulsed VCSELs is important for optical communications systems, as pulsed lasers are used for this application. Furthermore, in our experiments the laser is gain switched: the drive current is swept from well below threshold to above threshold on a nanosecond timescale, which should cause very large relaxation oscillations at the leading edge of the pulse. This is a drastically different operating regime from that observed in CW lasers, consequently it would not be surprising to observe different noise behavior. By varying the pulsewidth, we can observe how the noise changes when we move from regions where we expect the relaxation oscillations to last a significant fraction of the pulse duration to regions where they should be less important.

Furthermore, most previous noise measurements have involved the use of radio-frequency (RF) spectrum analysis, a technique that essentially measures the variance of the photocurrent fluctuations. To our knowledge all previous quantitative measures of polarization correlations have involved the determination of a correlation coefficient, which is also essentially a second-order moment of the intensity fluctuations. Here we have measured not just moments, but the full joint probability distributions for the fluctuations in two orthogonal laser polarizations. By measuring how the joint distributions and correlations change with the pulse duration we can infer whether the laser turn-on dynamics has any effect on polarization correlations in VCSELs, as turn-on more strongly influences the behavior of shorter pulses.

In our experiments we simultaneously detect the two orthogonal polarizations of the light emitted by a VCSEL. Each polarization output is incident on a separate photodetector, and we measure the number of photoelectrons generated in each detector as a function of drive current. The fact that we make simultaneous measurements on the two polarizations allows us to determine the full joint statistics. We find that in general the fluctuations in the orthogonal polarizations are anticorrelated, an observation that has been made previously by others and our-

#23232 - $15.00 US Received August 01, 2000; Revised September 25, 2000

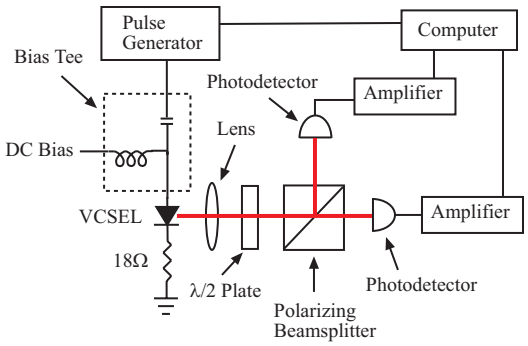

Fig. 1. The experimental apparatus.

selves [4-8,11]. However, we also find that the polarization correlations can be quite complicated. The joint distributions display considerable non-Gaussian structure, so measurements of second order moments are not enough to fully characterize the correlations.

2. Experiments

For these experiments we use a proton-implanted, gain-guided VCSEL with a peak emission wavelength of 837 nm; it has a 20 μm diameter, current-confined implant region, and an emission aperture of 15 μm. We drive the laser with short (3, 10, or 30 ns) current pulses at a pulse repetition frequency of 20 kHz; the rise and fall times of the pulses are 2.5 ns. We measure the laser drive current across an 18Ω resistor in series with the laser. The VCSEL has a DC bias of 1.38 V, which we apply through a bias tee. Biasing dramatically reduces ringing, and 1.38 V is the highest voltage we can apply without generating measurable CW background light from the laser; such background is found to increase the noise of our measurements [11].

As is shown in Figure 1, the light from the VCSEL is first collimated by a 10X, 0.25-N.A. microscope objective. It passes through a half-wave plate and then through a polarizing beamsplitter. We adjust the waveplate by driving the laser just above threshold and maximizing the 0° photodetector output. The laser operates in a single, linear polarization near threshold, so the direction of this polarization is what we refer to as 0°, while the orthogonal polarization is referred to as 90°. The light in each polarization exiting the beamsplitter is detected simultaneously by two photodetectors.

The details of our detection system and its calibration are discussed in Ref. [11]. The only difference between our current implementation and that of Ref. [11] is that we now use a 16-bit resolution A/D converter that simultaneously samples two detectors. This higher resolution digitization obviates the need for the biased amplifier we used previously. After calibration, this detection system yields the number of photoelectrons generated by each detector for each laser pulse. We expect this photoelectron number to accurately reflect the number of photons emitted by the laser to within our overall detection efficiency of over 80%. Since the detectors integrate over each pulse, we measure pulse-to-pulse statistics and do not resolve deterministic evolution or fluctuations within an individual pulse.

For each laser pulse width (3 ns, 10 ns, and 30 ns), we step through drive currents with values from below threshold to values of up to 6 times threshold. For the 30 ns pulses, we attenuate the laser output with a 0.3 neutral-density filter in order to avoid saturating our detectors at higher currents [17]. At each current value we simultaneously record the number of generated photoelectrons for each polarization (n_0 and n_{90}, where the subscripts refer to the polarization) for 10^6 pulses. From this data we generate two-dimensional histograms which represent joint probability distributions for the photoelectron numbers in the 0° and 90° polarizations. We use 128 bins along each coordinate, and the histogram bin widths are δn_0 and

#23232 - $15.00 US Received August 01, 2000; Revised September 25, 2000

δn_{90}. We normalize the histograms according to

$$\sum_{n_0}\sum_{n_{90}} P(n_0, n_{90})\delta n_0 \delta n_{90} = 1 \ , \tag{1}$$

so $P(n_0, n_{90})$ represents a joint probability density. These joint distributions, displayed as contour plots, provide a great deal of information about the correlations between the 0° and 90° outputs. Furthermore, from these distributions we calculate the marginal probability densities $P(n_0)$, $P(n_{90})$, $P(n_t)$, where the subscript t refers to the total number of photoelectrons $n_t = n_0 + n_{90}$. For example, the one-dimensional marginal distribution $P(n_{90})$ is given by the expression

$$P(n_{90}) = \sum_{n_0} P(n_0, n_{90})\delta n_0 \ . \tag{2}$$

We also calculate the mean $\langle n \rangle$ and variance $\langle (\Delta n)^2 \rangle$ of n_0, n_{90} and n_t.

To further quantify the correlations between the number of photoelectrons generated in the 0° and 90° polarizations, we calculate a correlation coefficient for these outputs at each drive current. The correlation coefficient is defined as

$$C_{0,90} = \frac{\langle (n_0 - \langle n_0 \rangle)(n_{90} - \langle n_{90} \rangle) \rangle}{\sigma_0 \sigma_{90}} = \frac{\langle n_0 n_{90} \rangle - \langle n_0 \rangle \langle n_{90} \rangle}{\sigma_0 \sigma_{90}} \ , \tag{3}$$

where σ_0 and σ_{90} are the standard deviations of the photoelectron output for each polarization. The correlation coefficient quantifies how the outputs in the two polarizations vary with respect to each other from pulse to pulse. It takes on values $-1 < C_{0,90} < 1$, with $C_{0,90} = 0$ corresponding to no correlation between the two outputs, $C_{0,90} = 1$ corresponding to perfect correlation, and $C_{0,90} = -1$ corresponding to perfect anticorrelation.

Another important parameter that describes the output of a laser which lases in more than one polarization is the polarization splitting ratio M [7,8]. For our laser M is given by

$$M = \frac{\langle n_{90} \rangle}{\langle n_0 \rangle} \ . \tag{4}$$

In order to determine the frequency structure of the transverse modes of the laser, we measured its spectrum with a scanning Fabry-Perot interferometer. This spectrum analyzer has a free spectral range (FSR) of 750 GHz and a finesse of greater than 280, yielding a resolution of 2.7 GHz. By placing the spectrum analyzer after the polarizing beamsplitter, with proper adjustment of the λ/2 plate we are able to sequentially measure spectra for each individual polarization output, and the total output. To measure the spectrum of the total output, we rotate the half-wave plate halfway between the settings used to measure the two individual polarizations. Thus, each laser polarization is incident on the polarization axis of the beamsplitter at 45°, and we effectively measure half the output from each polarization. We collect spectra as a function of the laser drive current, and use this data to determine the number of lasing modes at each drive current.

3. Results for 10 ns pulses

Figure 2(a) shows the mean number of detected photoelectrons $\langle n \rangle$ plotted as a function of laser drive current for 10 ns current pulses; these plots are essentially the LI (light-current) curves for our laser. We plot $\langle n \rangle$ for each polarization and the total. As can be seen from the figure, the light output does not increase linearly with current but rather has kinks. Such behavior has been observed before, and these kinks correspond to points where an additional

#23232 - $15.00 US Received August 01, 2000; Revised September 25, 2000

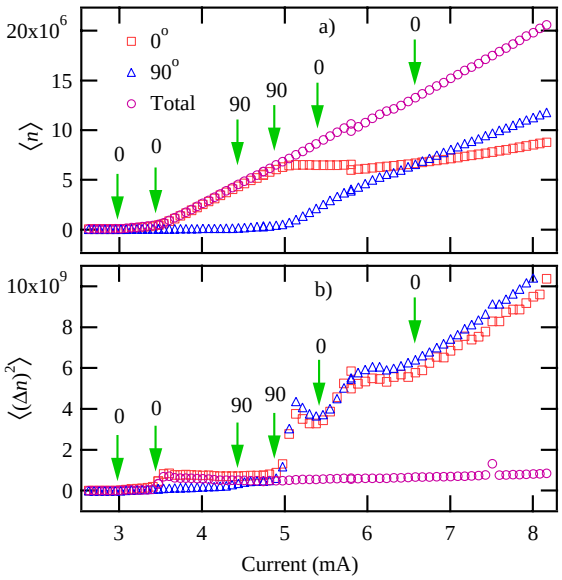

Fig. 2. Plot of the mean (a) and variance (b) of the number of photoelectrons as a function of drive current for 10 ns pulses. Data is shown for the individual polarizations and the total output. Arrows indicate current values where new modes turn on, and are labeled by the polarization of the new mode.

mode comes above its threshold [2,11]. The arrows in Fig. 2 indicate current values where a new laser mode comes above threshold; these points were determined by examining the laser spectra. At each arrow one new mode comes above threshold, and we have labeled the polarization of the new mode (0° or 90°) at the arrow. Thus, there's one mode lasing in the 0° polarization between 3.0 and 3.4 mA, while there are two modes in the 0° polarization and two modes in the 90° polarization between 4.9 and 5.4 mA. Above 6.6 mA it becomes difficult to resolve the mode structure, and the best we can say is that there are 6 or more modes lasing.

In Fig. 2(b) we plot the variance of the detected photoelectrons $\left\langle (\Delta n)^2 \right\rangle$ as a function of laser drive current for 10 ns current pulses, again showing data for each polarization and the total. It can be seen that there are sudden increases in the photon variance when new modes turn on. Such increases have been observed before, and are associated with increases in mode partition noise with the turn-on of additional modes [4,11]. Another interesting feature of Fig. 2(b) is that $\left\langle (\Delta n)^2 \right\rangle$ is larger for the individual polarizations than it is for the total output. The only way this can occur is if the outputs in the two polarizations are anticorrelated. This behavior has been observed previously by us and by others, and can be explained as competition between modes in the two polarizations for a fixed amount of gain [4-8,11]. The total output is fixed by the total available gain, but the distribution of this output between the two polarizations is not so tightly constrained. Thus, the total output fluctuates less than the outputs in the individual polarizations.

The primary purpose of these experiments is to explore in more detail the correlations between the laser polarizations. As described above, we accomplish this by examining the joint probability density $P(n_0, n_{90})$ that there will be n_0 photoelectrons generated in the detector monitoring the 0° polarization and n_{90} photoelectrons in the detector monitoring the 90° polarization. Fig. 3 shows an example of a typical two-dimensional distribution and its relationship to the 1-dimensional marginal distributions. The 1D distribution for the 90° polarization

#23232 - $15.00 US
Received August 01, 2000; Revised September 25, 2000

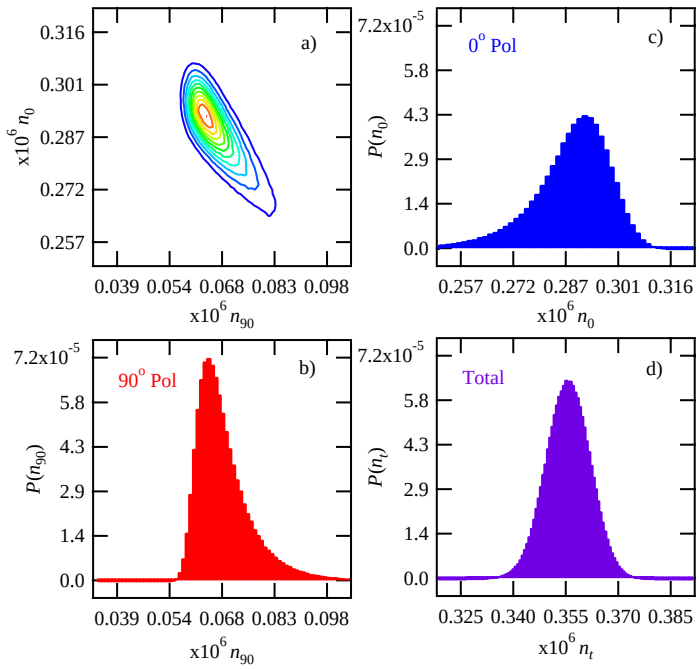

Fig. 3. Distributions at a drive current of 3.3 mA (one mode lasing) for 10 ns pulses: a) joint distribution $P(n_0, n_{90})$, b) distribution for the 90° output, c) distribution for the 0° output, d) distribution for the total output.

$P(n_{90})$ can be formed by integrating out the 0° information, that is by summing along vertical lines in Fig. 3(a) and essentially projecting $P(n_0, n_{90})$ onto the horizontal axis [Eq. (2)]. This distribution is plotted in Fig. 3(b). Similarly, $P(n_0)$, Fig. 3(c), can be formed by integrating out the 90° information (i.e., projecting the 2D distribution onto the vertical axis.) It so happens that the distribution for the total output $P(n_t)$, Fig. 3(d), can be found by integrating along lines that make a slope of -1 in Fig. 3(a), and thus projects the joint distribution onto an axis that makes a 45° angle.

The shapes of the 2D joint distributions give direct evidence for anticorrelation between the 0° and 90° outputs, as we find that above threshold these distributions lie primarily along a line whose slope is –1. Anticorrelation tells us that light pulses that have a higher n_{90} will tend to have a lower n_0, and vice versa. This is shown clearly in Fig. 4(a); at this drive current of

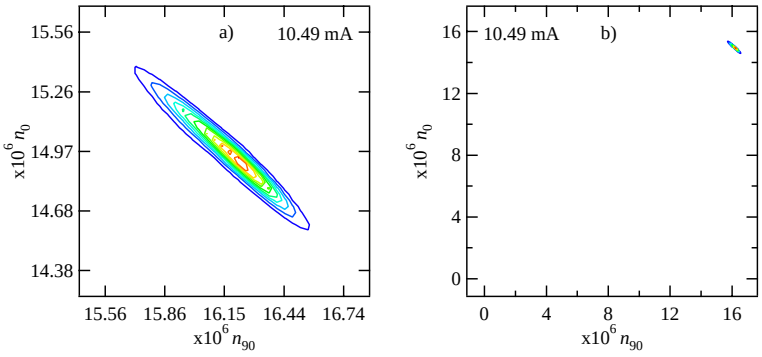

Fig. 4. [a) 1.4 MB, b) 600 KB] Animation of $P(n_0, n_{90})$ as a function of drive current for 10 ns pulses: a) closeup of the shape of the distributions, b) all distributions shown on the same scale.

#23232 - $15.00 US
Received August 01, 2000; Revised September 25, 2000

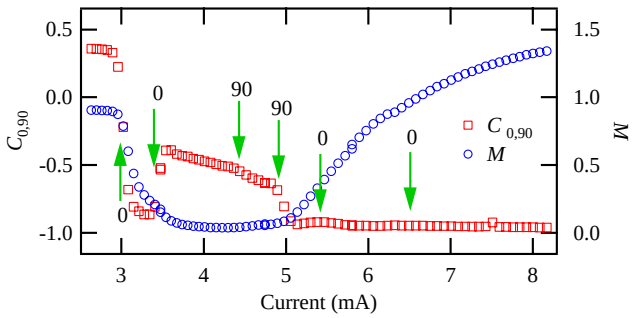

Fig. 5. The correlation coefficient and polarization splitting ratio are plotted as a function of laser drive current for 10 ns pulses. Arrows indicate current values where new modes turn on, and are labeled by the polarization of the new mode.

10.5 mA there are more than six modes lasing, and the anticorrelations are very strong.

We have also constructed animations of the 2D joint distributions, displayed with increasing drive current in time; these are shown in Fig. 4. The animations show how the distributions change in size, shape, and position with increasing drive current. Figure 4(a) shows how the shape of the distributions change with drive current. It will be noticed that at lower currents, corresponding to small numbers of lasing modes, the distributions tend to be asymmetric and can be non-Gaussian. However, at larger currents the distributions become symmetric Gaussian distributions, which lie predominantly along a line whose slope is –1, which indicates strong anticorrelation between the polarization outputs. We notice that at certain currents there are qualitative changes in the shape of the distributions. By comparing with Fig. 2, we find that these changes usually occur at currents where a new mode comes above threshold.

Figure 4(b) shows animations that are derived from exactly the same data as in Fig. 4(a), but the frames are plotted on a much larger scale. Here the scale is large enough to include the entire evolution of the distributions, from the smallest current to the largest. This figure illustrates how the mean number of photoelectrons $\langle n \rangle$ changes in each polarization, as well as how the size of the distribution changes, as a function of drive current. The drawback to this animation is that at low drive currents the distributions themselves are so small that they can barely be seen. For full benefit of Fig. 4, both animations should be played simultaneously, side by side.

Figure 5 shows a plots of the correlation coefficient $C_{0,90}$ and the polarization spliting ratio M as functions of the drive current for 10 ns pulses. Again, arrows indicate currents where new modes come above threshold. As can be seen, when the laser is below threshold the two polarizations are slightly positively correlated. We believe that this is due to small fluctuations in the pump current; such fluctuations would affect the number of emitted photons in both polarizations in the same way, and thus the two outputs would be positively correlated.

Once the laser comes above threshold (in the 0° polarization) at 3.0 mA, the correlation coefficient drops dramatically and the two polarizations become anticorrelated. However, when the second mode turns on at 3.4 mA (also in the 0° polarization), the outputs become less anticorrelated. When the third mode (the first in the 90° polarization) turns on at 4.5 mA, the output becomes slightly more anticorrelated, and when the fourth mode (the second 90°) turns on at 4.9 mA the output becomes significantly more anticorrelated, approaching a perfect anticorrelation of $C_{0,90} = -1$.

With the exception of the region in which only a single mode is lasing (drive currents between 3.0 and 3.4 mA), there seems to be a correspondence between M and $C_{0,90}$; smaller polarization imbalance (M approaches 1) corresponds to stronger anticorrelation, as predicted for CW lasers in Ref. [7]. In this reference it was theoretically predicted that the correlation

#23232 - $15.00 US
Received August 01, 2000; Revised September 25, 2000

coefficient should approach -1 when the polarization splitting ratio approaches 1. However, we do not fully understand why the anticorrelations become weaker when two or three modes are lasing (between 3.4 and 5.0 mA). One possible explanation is that at this point much more light is being emitted in the 0° polarization (notice the low value of the polarization splitting ratio at these drive currents in Fig. 5.) The relatively high output in the 0° polarization causes much larger fluctuations in this polarization than in the 90° polarization [as seen in Fig. 4a).] Thus, the 90° fluctuations are unable to compensate for the 0° fluctuations and the anticorrelation between the two outputs decreases. In other words, there simply isn't enough intensity in the 90° polarization to develop any significant correlation. This explanation is not completely satisfactory, however, because one may expect a correspondingly abrupt change in the polarization splitting ratio to accompany the change in the amount of correlation, but Fig. 5 does not indicate an abrupt change in *M*.

There is another way to look at this problem as well. Imagine that the correlations when only a single mode is lasing were closer to -0.3 instead of -0.8. If this were true, there would be a monotonic decrease in the correlation coefficient towards -1 as the laser was driven higher above threshold. The question then becomes not why do the anticorrelations decrease when the second mode turns on, but rather why are the anticorrelations so strong when only a single mode is lasing? In this case only one polarization is lasing, but it has rather strong anticorrelations with nonlasing modes. Again, we do not have a detailed answer to this question, but we assume that the anticorrelations come from the fact that the lasing and nonlasing modes are competing for the same gain, so will show anticorrelation. We also point out that other authors have seen similarly strong anticorrelations between lasing and nonlasing modes [4,8].

Figure 5 clearly shows that the number of lasing modes in this laser dramatically affects the polarization correlations, since abrupt changes in the correlation coefficient occur at currents where new laser modes come above threshold. This is consistent with the observations made regarding Fig. 4 in which qualitative changes in the shape of the joint distributions are associated with changes in the number of lasing modes. Such dramatic changes in the amount of correlation were not predicted by the model of Ref. [7], however this is not necessarily surprising. The model of Ref. [7] treated only two polarization modes, and did not include the effects of multiple transverse modes contained within each polarization.

4. Results for other pulse widths

In addition to studying 10 ns pulses, we repeated the above-described experiments with drive-current pulse widths of 3 and 30 ns. Differences in the behavior of the laser between these three pulse widths indicate how the laser behaves on different time scales. The pulse durations that we have used are long compared to the photon lifetime in the cavity (a few picoseconds), but the shorter pulses we have used are of comparable duration to the carrier lifetime in the cavity (a few nanoseconds). Probably the most relevant timescales are the period of the relaxation oscillations, T_{ro}, and the damping of the relaxation oscillations, τ_{ro}. While we have not directly measured these timescales in our laser, we expect them to be on the order of 0.1-1 ns for T_{ro}, and on the order of 1 ns for τ_{ro} [8]. Because we are gain switching these lasers, we expect large relaxation oscillations will be present for much of the 3 ns pulses, but will be present only at the beginning of the 30 ns pulses.

In Fig. 6 we show animations of the joint probability densities $P(n_0, n_{90})$ for 3 and 30 ns duration pulses. Because shorter pulses contain fewer photons, we were able to drive the 3 ns pulses higher above threshold than the longer pulses without saturating the detectors, and it can be seen that at higher drive currents the joint distributions for the 3 ns long pulses take on some interesting shapes. By comparing the shapes of the distributions for the three different pulse widths closer to threshold, we see that the distributions for shorter pulses tend to have more irregular shapes, while those of the longer pulses tend to be smoother. We have no good

#23232 - $15.00 US Received August 01, 2000; Revised September 25, 2000

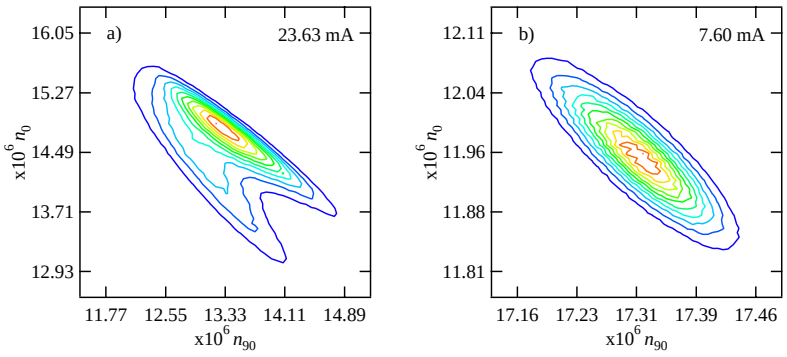

Fig. 6. [a) 980 KB, b) 850 KB] Animation of $P(n_0, n_{90})$ as a function of drive current: a) 3 ns duration pulses, b) 30 ns duration pulses.

explanation for the shapes of the distributions that we observe, and can only suggest that they are somehow related to relaxation oscillations at the beginning of the pulse, which more strongly affect the 3 ns pulses. A detailed numerical model would be likely be necessary to explain this observed behavior.

We find that as the pulse width changes, so does the amount of polarization correlation. In Fig. 7 we plot the correlation coefficient and the polarization splitting ratio for each pulse width as a function of normalized current (drive current divided by the threshold drive current). As can be seen from Fig. 7, all pulse widths display roughly the same qualitative behavior. With the exception of the region in which only a single mode is lasing (between about 1.0 and 1.1 times threshold), there seems to be a correspondence between M and $C_{0,90}$; smaller polarization imbalance (larger M) corresponds to stronger anticorrelation, as predicted in Ref. [7]. In the region between about 1.2 and 1.7 times threshold, it is seen that the polarization anticorrelations are stronger for shorter pulses. We don't have a full explanation of why the correlations are pulse width dependent. In addition to differences in the influence of relaxation oscillations for different pulse widths, it has been observed that different transverse modes can

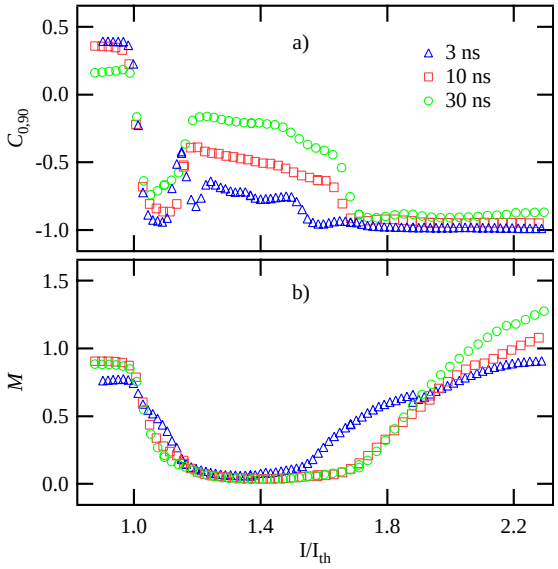

Fig. 7. The correlation coefficient (a) and the polarization splitting ratio (b) are plotted as a function of normalized drive current for three different pulse durations.

#23232 - $15.00 US
Received August 01, 2000; Revised September 25, 2000

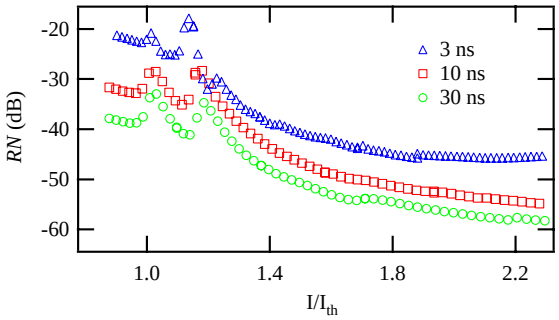

Fig. 8. The relative noise is plotted as a function of normalized drive current for three different pulse durations.

turn on at different times during pulsed excitation [16]. We were not able to time resolve the behavior of individual modes in our laser. It is thus possible, for instance, that certain modes may contribute strongly to the behavior of the 3 ns pulses, while other modes which turn on later are more important in the 30 ns pulses. Models which treat CW lasers by assuming small fluctuations about a steady state solution are unlikely to be adequate to explain the variation of $C_{0,90}$ with pulsewidth [7,8]. Once again, a numerical model which accurately treats the transient effects encountered during gain switching is probably necessary to explain this behavior.

We have chosen to use a normalized horizontal scale when comparing different pulse widths because while the 10ns and 30 ns pulses have similar threshold currents, the 3 ns pulses have a higher threshold current. This observed higher threshold current for the shorter pulses may be an artifact resulting because the rise and fall times of our pulses are approximately 2.5 ns, which means that the 3 ns current pulses are not square. This makes the absolute amplitude of the 3 ns current pulses difficult to determine precisely. Normalizing the drive current by the observed threshold drive current eliminates this problem, and makes for appropriate comparisons between different pulse widths.

In Fig. 8, we plot the relative noise *RN* of the laser output as a function of the normalized current for the three different pulsewidths. The relative noise is defined as [11]

$$RN = \frac{\langle (\Delta n_t)^2 \rangle}{\langle n_t \rangle^2} \quad . \tag{5}$$

As can be seen, the shorter pulses tend to be noisier. One possible explanation for this is that the relaxation oscillations increase the noise early in the pulse; when these transients die out the pulse displays lower-noise, more steady state operation. Thus, shorter pulses for which the relaxation oscillations make up a more significant fraction of the pulse duration will have larger relative noise than longer pulses.

5. Conclusions

We have measured the polarization correlations of a pulsed VCSEL. Above threshold, the outputs in the orthogonal, linear polarizations of the laser are anticorrelated. We also find that the degree of correlation depends primarily upon the number of lasing modes. Anticorrelation is greatest when a) the outputs in the two polarizations are of similar amplitude and b) many modes are lasing. These criteria are plausible because anticorrelation depends upon competition between the modes of the two polarizations. A very weak output cannot compete well with a strong output. Also, mode competition that leads to anticorrelation depends upon spatial and temporal overlap of the modes in the laser. The more modes that are lasing in the two polariza-

#23232 - $15.00 US
Received August 01, 2000; Revised September 25, 2000

tions, the more likely these modes are to overlap and affect each other through spatial hole burning [18].

Although we can quantify the polarization correlations by the correlation coefficient $C_{0,90}$, we find that this is a drastic oversimplification of the problem. The correlation coefficient is derived from second order moments of the joint probability density for the polarization fluctuations $P(n_0, n_{90})$. For Gaussian statistics moments up to second order can fully characterize the fluctuations; to a good approximation this is the case for our laser when it is between 1.8 and 5 times above threshold. However, closer to threshold we find that the statistics are not Gaussian (Figs. 4 & 6), and the correlations are of a much more complicated form.

We also have indirect evidence that the noise of the laser changes in time. This comes from the observation that the relative noise of shorter laser pulses is larger than that of longer laser pulses. This behavior suggests larger noise right after the laser turns on, followed by quieter operation thereafter. This behavior is likely to be caused in part by relaxation oscillations at the leading edge of the pulse. It has also been previously observed that individual transverse modes in a VCSEL can turn on and off at different times during the pulse [16], which might further explain our observations. Modes may be turning on and off over time in our laser, but the measurements we have made would not be able to see this effect. In order to more fully describe this behavior, experiments that better time-resolve the fluctuations and the laser mode structure are necessary.

Acknowledgments

This research was supported by the National Science Foundation and Research Corporation.

#23232 - $15.00 US Received August 01, 2000; Revised September 25, 2000